PHYSICAL REVIEW D **87,** 043511 (2013)

CMB maximum temperature asymmetry axis: Alignment with other cosmic asymmetries

Antonio Mariano*
Department of Mathematics and Physics, University of Salento, Via Arnesano, 73100 Lecce, Italy

Leandros Perivolaropoulos†
Department of Physics, University of Ioannina, 45110 Ioannina, Greece
(Received 30 November 2012; published 5 February 2013)

We use a global pixel-based estimator to identify the axis of the residual Maximum Temperature Asymmetry (MTA) (after the dipole subtraction) of the WMAP seven-year Internal Linear Combination (ILC) cosmic microwave background temperature sky map. The estimator is based on considering the temperature differences between opposite pixels in the sky at various angular resolutions (4°–15°) and selecting the axis that maximizes this difference. We consider three large-scale HEALPix resolutions: $N_{\rm side} = 16(3.7°)$, $N_{\rm side} = 8(7.3°)$ and $N_{\rm side} = 4(14.7°)$. We compare the direction and magnitude of this asymmetry with three other cosmic asymmetry axes (α dipole, dark energy dipole and dark flow) and find that the four asymmetry axes are abnormally close to each other. We compare the observed MTA axis with the corresponding MTA axes of 10^4 Gaussian isotropic simulated ILC maps (based on ΛCDM). The fraction of simulated ILC maps that reproduce the observed magnitude of the MTA asymmetry and alignment with the observed α dipole is in the range of 0.1%–0.5% (depending on the resolution chosen for the cosmic microwave background map). The corresponding magnitude + alignment probabilities with the other two asymmetry axes (dark energy dipole and dark flow) are at the level of about 1%. We propose Extended Topological Quintessence as a physical model qualitatively consistent with this coincidence of directions.

DOI: 10.1103/PhysRevD.87.043511 PACS numbers: 98.80.Es, 98.62.Sb, 98.65.Dx

I. INTRODUCTION

There is observational evidence coming mainly from the isotropy of the cosmic microwave background (CMB) that the Universe is isotropic on Hubble scales. Any anisotropy on these scales is bound to be smaller than about 1 part in 10^3. This constraint, combined with the Copernican principle (supported by kSZ data [1]), leads to strong support of the cosmological principle: the Universe is homogeneous and isotropic on Hubble scales.

Violation of the cosmological principle is expected to occur at a small level even on Hubble scales due to small statistical fluctuations of the cosmic energy density (matter, radiation, dark energy). Precise cosmological observations are in principle able to detect this deviation from the cosmological principle on Hubble scales and compare the expected magnitude with the one anticipated based on the standard isotropic cosmological model.

The lowest-order deviation from isotropy, which is also easiest to detect, is the anisotropy that distinguishes a preferred cosmological axis. Such an axis is usually reasonably described by a dipole deviation from isotropy. The dipole asymmetry corresponds to the component of the CMB maps described by the function $T(\theta) = A\cos\theta$, where A is the dipole magnitude and θ is the angle with the dipole axis defined as the axis that maximizes the value of A. In the case of the CMB temperature perturbations, the dipole term is dominated by our motion with respect to the CMB frame, and therefore it has been removed completely from the CMB maps. This removal has also swept away any subdominant cosmological contribution to the dipole. However, any axial cosmological anisotropy that is not perfectly described by a dipole could have left a trace after the removal of the dipole. For example, Hubble-scale inhomogeneities with appropriate geometries could induce multipole axial asymmetries (l, $m = 0$) of the form $T(\theta) = C_l(\cos\theta)^l$ ($l > 1$). After the subtraction of the dipole, such asymmetries remain unaffected and could be detected with properly designed statistical tests. The statistical test we will be using in the analysis of the CMB maps can pick up, for example, the combined effect of such leftover higher-multipole axial asymmetries with odd l, even after the dipole has been subtracted. It could also pick up other leftover axial asymmetries that may not be described by higher multipoles.

Early hints for deviations from isotropy on Hubble scales have been accumulating during the last decade. Some of these hints may be summarized as follows [2,3]:

(1) *Large-scale velocity flows (dark flow):* There are recent indications that there is a large-scale peculiar velocity flow with amplitude larger than 400 km/sec on scales up to $100h^{-1}$Mpc($z \leq 0.03$) [4] with direction $l \simeq 282° \pm 11°$, $b \simeq 6° \pm 6°$. Other independent studies have also found large bulk velocity flows with similar direction [5] on scales of about $100h^{-1}$ Mpc or larger than $300h^{-1}$ Mpc [6].

*antonio.mariano@le.infn.it
†leandros@uoi.gr

This large-scale peculiar velocity flow is known as *dark flow*. The standard homogeneous isotropic cosmology (ΛCDM) predicts significantly smaller amplitude and scale of flows than what these observations indicate. The deviation of these observations from ΛCDM predictions is more than 3σ. Other studies [7] using type-Ia supernovae find a flow of a somewhat smaller magnitude, consistent with ΛCDM. Even in these studies, however, the direction of the flow is similar to the direction found by Refs. [4,6]. Thus, even though there is some controversy about the magnitude of the dark flow, it appears that its direction is more robust even though its directional 1σ error region is probably larger than the one indicated in Ref. [4]. (For a more conservative 1σ error region, see Ref. [7].) A possible connection of large-scale velocity flows and cosmic acceleration may be found in Ref. [8].

(2) *Fine structure constant* (α) *dipole:* Quasar absorber spectra obtained using UVES (the Ultraviolet and Visual Echelle Spectrograph) on the VLT (Very Large Telescope) in Chile, and also previous observations at the Keck Observatory in Hawaii [9], have indicated that the value of the fine structure constant at high redshifts ($z \in [0.2, 4.2]$) is not distributed isotropically. Its anisotropy is well described by a dipole with its axis directed towards $l \simeq 320^\circ \pm 11^\circ$, $b \simeq -11^\circ \pm 7^\circ$. The deviation of these observations from isotropy is 4.1σ [9,10].

(3) *Dark energy dipole:* A recent fit of the type-Ia distance moduli residuals (from the best-fit ΛCDM) to a dipole anisotropic distribution has indicated [10] that the angular distribution of these residuals is well described by a dipole analogous to the fine structure constant dipole. Its axis is towards $l \simeq 309^\circ \pm 18^\circ$, $b \simeq -15^\circ \pm 11^\circ$ and deviates by only about 11° from the fine structure constant dipole. The deviation of these observations from isotropy is at the 2σ level.

Each one of the above observed deviations from isotropy is between 2σ and 4σ. The angular proximity of the corresponding anisotropy axes makes their combination even more unlikely in an isotropic universe where there is no correlation between them. In Ref. [10], it was shown that the combined magnitude + alignment of the fine structure constant α and dark energy dipoles has a probability less than one part in 10^6 to occur in an isotropic universe where the two dipoles are uncorrelated.

A physical model was proposed in Refs. [10,11] that has the potential to explain the existence and the alignment of the above three dipoles. The model is based on the existence of a topological defect (e.g., a global monopole) with a Hubble-scale core formed during a recent phase transition by an $O(3)$ symmetric scalar field *nonminimally coupled to electromagnetism*. An off-center observer with respect to the monopole center would observe faster accelerating expansion towards the core where the vacuum energy density is larger, and also varying α along the same direction due to the variation of the scalar field magnitude. This model is a generalization of "topological inflation" [12] and has been called *extended topological quintessence* [10] due to its nonminimal coupling to electromagnetism. The model also has some similarities with texture models which have been considered as a physical origin of the observed cold spots on CMB maps [13]. In contrast to extended topological quintessence, however, texture models have not been considered as a possible physical origin for cosmic accelerated expansion or for the spatial variation of α.

Extended topological quintessence makes the following qualitative predictions [10]:

(i) *Large-scale velocity flows:* Due to the stronger repulsive gravity in the defect core, a large-scale peculiar velocity flow is predicted along the axis that connects the off-center observer and the monopole core. The direction of the flow is predicted to be away from the repelling core ("Great Repulser"), and its scale is predicted to be the Hubble scale (the defect core scale). A reversal of the velocity flow direction is predicted for observations that go beyond the defect core. As discussed in the following section, the direction of the observed dark flow is consistent with the directions of the fine structure and dark energy dipoles in accordance with the above prediction.

(ii) *Correlation between values of α and presence of strong magnetic fields:* As discussed in Ref. [10], the scalar field magnitude is expected to depend weakly on the presence of local strong magnetic fields. This magnitude variation is in turn expected to lead to local variations of α in cosmological regions with large magnetic fields.

(iii) *Maximal large-scale CMB variation towards the defect core:* Due to the recent formation of the global defect, the ISW effect is expected to lead to large temperature differences between opposite directions in the sky along the direction towards the defect core. A large part of this temperature asymmetry would have been subtracted from CMB maps along with the dipole moment, which is mainly due to our motion with respect to the CMB. However, smaller traces of this asymmetry could have survived the dipole subtraction and may be detectable in large-scale CMB maps.

A wide range of *large-scale anomalies* have been detected on CMB maps [14,15]. The anomalies include an abnormal alignment and planarity of the octupole and quadrupole moments [16,17], the existence of two large and deep cold spots [18–20], the lack of large-scale power [21–24], the even excess of the CMB power spectrum [25],

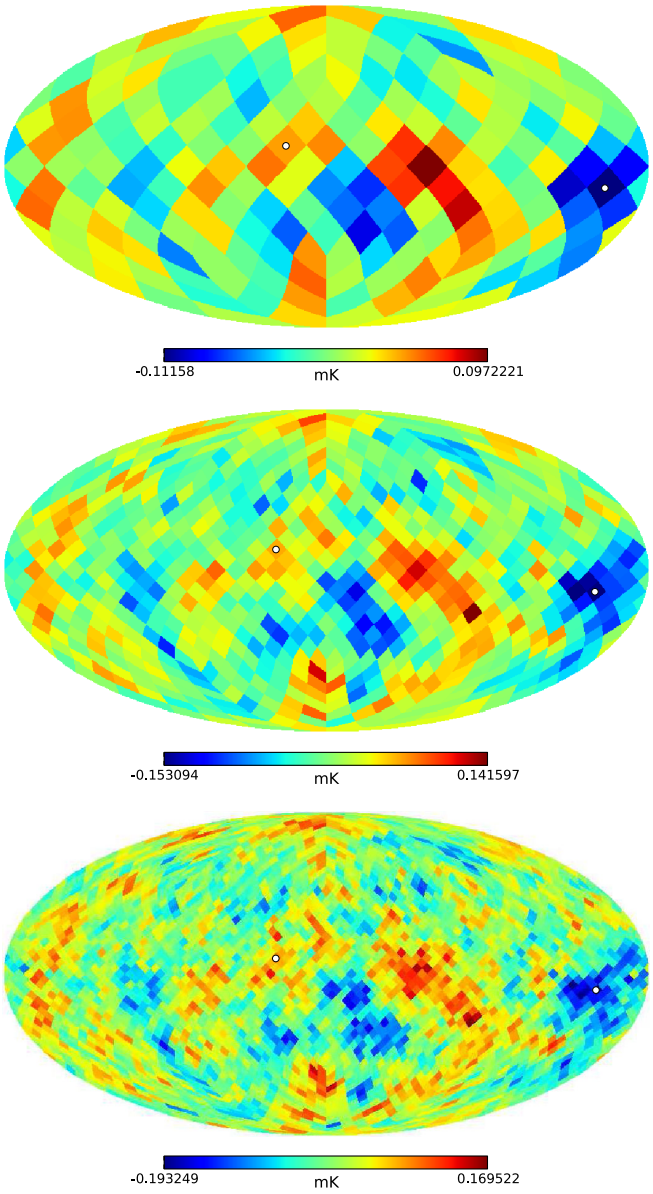

FIG. 1 (color online). Degraded temperature maps obtained from the seven-year ILC CMB map with $N_{\rm side} = 4$, 8, 16. The white dots define the maximum temperature differences direction.

the hemispherical power asymmetry [26] and quadrupolar dependence of the two-point function (see Ref. [15] for a detailed review). Recent evidence for mirror symmetry and antisymmetry (along different directions) has also been obtained [27,28] using the ILC WMAP7 CMB map [29]. Finally, evidence for the existence of statistically significant giant rings in the CMB sky has also been reported [30]. Some of these anomalies appear to be related to a large-scale bipolar asymmetry of the CMB, even though there is no current quantitative study of a physical model than can give rise to all these anomalies simultaneously (see, however, Refs. [13,31–33]). Due to the lack of such a model, these anomalies are usually assumed to be *a posteriori* manifestations of expected large statistical fluctuations.

TABLE I. Directions in galactic coordinates for the α [9,10] and dark energy dipoles [10], the dark flow and the maximum CMB temperature difference (MTA). For the dark flow direction, we have used Ref. [4]. The larger-scale direction of Ref. [6] is consistent with that of Ref. [4], but it has significantly larger error bars. The error on the MTA direction has been taken to be equal to the side of the pixel, $\sqrt{4\pi/(12N_{\rm side}^2)}$ rad.

	l (°)	b (°)
MTA ($N_{\rm side} = 4$)	337.5 ± 14.7	-9.6 ± 14.7
MTA ($N_{\rm side} = 8$)	331.9 ± 7.3	-9.6 ± 7.3
MTA ($N_{\rm side} = 16$)	331.9 ± 3.7	-7.2 ± 3.7
α dipole	320.5 ± 11.8	-11.7 ± 7.5
Dark energy dipole	309.4 ± 18.0	-15.1 ± 11.5
Dark flow direction	282 ± 11	6 ± 6

Having at our disposal a well-defined physical model which makes specific predictions allows us to focus on specific aspects of CMB maps and search for signatures of our model. Thus, in what follows, we focus on the predicted large-scale CMB anisotropy and search for the axis of maximal temperature asymmetry in the WMAP7 ILC map. In particular, we consider three large-scale HEALPix pixelizations [34] of the WMAP7 ILC map and identify those pairs of opposite pixels in the sky that correspond to Maximum Temperature Difference. We compare the magnitude of this maximum temperature asymmetry (MTA) with that expected from an isotropic model using Gaussian simulated CMB maps. We also compare the direction of the MTA with the direction of the other observed cosmic asymmetry axes (dark flow, dark energy dipole and α dipole). We find the likelihood that the observed magnitude and alignment would occur by chance in an isotropic model with no correlation between the CMB and the other observables.

The structure of this paper is the following: In the next section, we describe in some detail the method for identifying the MTA magnitude and direction in the WMAP7 ILC map. We also show the resulting magnitude and direction, as well as its alignment with the other observed axes. We then compare the observed magnitude and alignment with those obtained by 10^4 Gaussian simulated ILC maps based on ΛCDM. In Sec. III, we discuss the implications of our results and point out the next steps of this research program.

II. METHOD AND RESULTS

The subtraction of the dipole moment from the CMB maps removes, along with the dominant Doppler component, any cosmological signal that may happen to have a dipole anisotropy. Such a signal is expected to emerge in the context of extended topological quintessence, as discussed in the Introduction (see also Refs. [10,11]). In addition to the dipole, however, an off-center observer

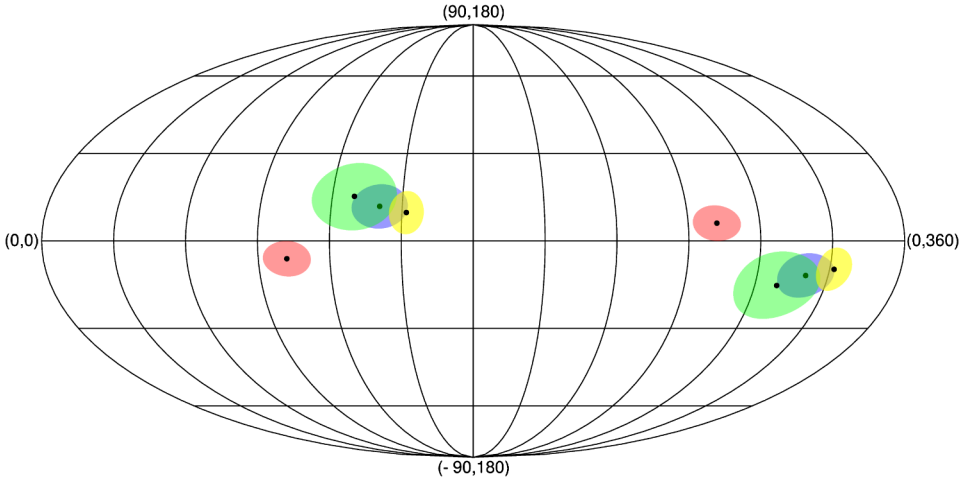

FIG. 2 (color online). Directions in galactic coordinates for the α [blue (second shaded region starting from right)] and dark energy [green (third shaded region starting from right)] dipoles, for the dark flow direction [red (fourth shaded region starting from right)] and for the direction of MTA in the seven-year ILC CMB map degraded to $N_{\rm side} = 8$ [yellow (first shaded region starting from right)]. The opposite corresponding directions are also shown.

will also experience axial anisotropies corresponding to higher moments, although at a smaller magnitude [35,36]. Depending on the dynamics and the geometry of the forming defect, these higher-moment asymmetries may have detectable magnitude. Such asymmetry could manifest itself as maximized temperature difference between opposite pixels in the CMB sky. In order to obtain the direction and magnitude of such residual MTA, we use the following steps, applied on the WMAP7 foreground-reduced ILC map pixelized according to HEALPix. In order to minimize foreground contamination, we focus on large angular scales: $N_{\rm side} = 4$ (pixel size about 14.7°), $N_{\rm side} = 8$ (pixel size about 7.3°), $N_{\rm side} = 16$ (pixel size about 3.7°):

(1) We construct a temperature difference map (TDM), which is obtained by assigning to each pixel a number equal to the difference between its temperature value and the value of the temperature of the opposite pixel in the sky. Thus we have

$$D^{-}(\hat{n}_i) = (T(\hat{n}_i) - T(-\hat{n}_i)), \qquad (2.1)$$

where $\hat{n}_i$ is the direction of the ith HEALPix pixel. A similar estimator was considered in Ref. [37] in an effort to test the statistical isotropy of CMB maps. In the context of the HEALPix pixelization, the opposite pixel is always simply defined and identified. By construction, opposite pixels of the TDM are assigned to opposite values.

(2) In the TDM, we select the pixel $D^{-}_{\rm max}(\hat{n}_k)$ with the maximum absolute value. This pixel, along with the pixel located opposite to it, defines the axis of MTA. If the dipole had not been subtracted, the MTA axis would be almost identical to the dipole axis. Thus, the MTA axis is the residual asymmetry axis after the subtraction of the dipole.

(3) The direction of the MTA is then compared with the directions of other cosmic asymmetry axes (α dipole, dark energy dipole and dark flow), and the corresponding angular differences are identified.

(4) The magnitude and direction of the MTA are compared with a large number of ΛCDM simulated ILC maps [38], and we evaluate the likelihood of obtaining the observed MTA magnitude (or larger) in the context of ΛCDM. The likelihood of obtaining the angular differences (or smaller) with the other cosmic asymmetry axes in the context of ΛCDM is also evaluated.

The WMAP7 ILC maps using HEALPix pixelizations with $N_{\rm side} = 4, 8, 16$ [corresponding to a pixel size of

TABLE II. Angular distances in degrees between the α and dark energy dipoles, the dark flow and the MTA directions. For the MTA direction we have chosen the result obtained in the $N_{\rm side} = 8$ case.

	MTA	α dipole	DE dipole	DF direction
MTA ($N_{\rm side} = 8$)	0.0	11.4 ± 12	22.6 ± 18	52.1 ± 11
α dipole	11.4 ± 12	0.0	11.3 ± 18	42.2 ± 11
DE dipole	22.6 ± 18	11.3 ± 18	0.0	34.4 ± 18
DF direction	52.1 ± 11	42.2 ± 11	34.4 ± 18	0.0

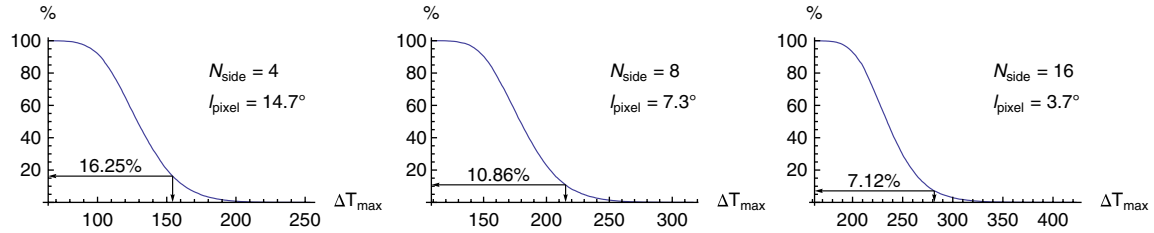

FIG. 3 (color online). Percentage of the maximum temperature difference values obtained from the simulated maps that is bigger than the observed maximum temperature difference obtained from the degraded maps with $N_{side} = 4, 8, 16$.

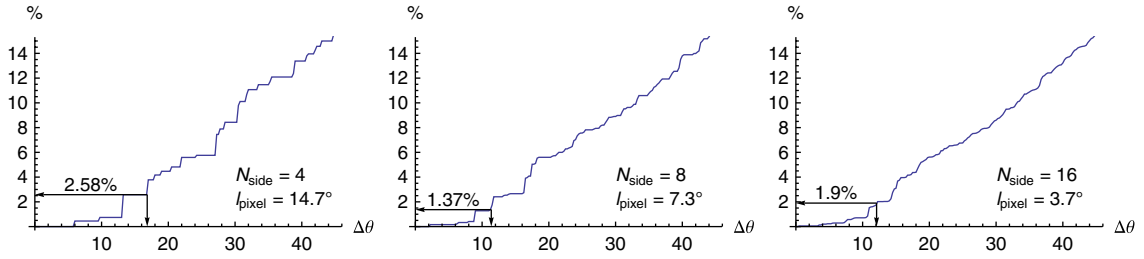

FIG. 4 (color online). Percentage of the maximum temperature difference directions obtained from the simulated maps closer to the α dipole than the observed maximum MTA obtained from the degraded maps with $N_{side} = 4, 8, 16$.

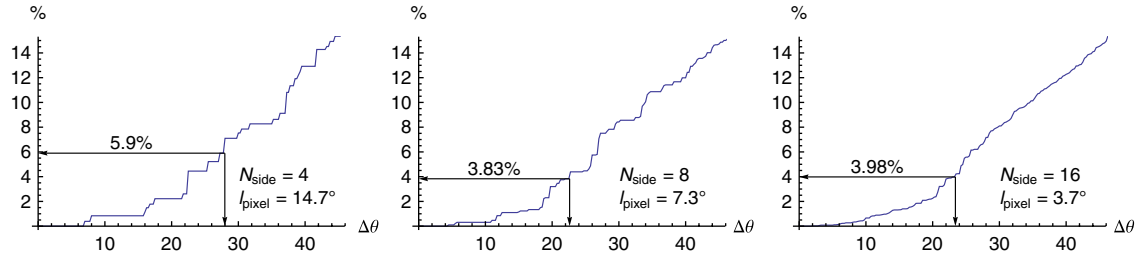

FIG. 5 (color online). Percentage of the MTA directions obtained from the simulated maps closer to the dark energy dipole than the observed MTA directions obtained from the degraded maps with $N_{side} = 4, 8, 16$.

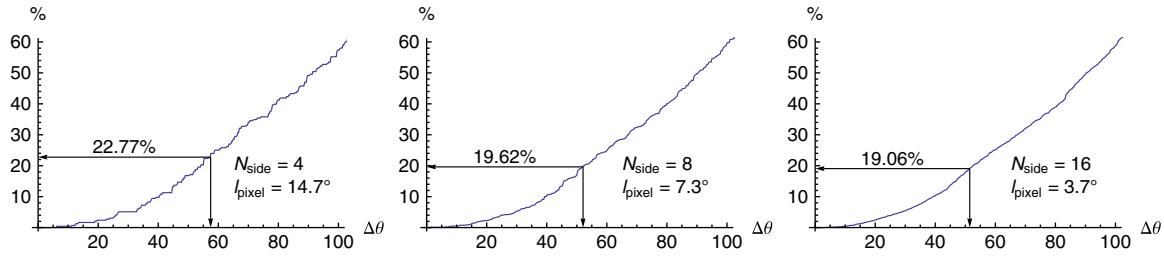

FIG. 6 (color online). Percentage of the MTA directions obtained from the simulated maps closer to the dark flow direction than the observed MTA directions obtained from the degraded maps with $N_{side} = 4, 8, 16$.

$\sqrt{4\pi/(12N_{side}^2)}$ rad; i.e., about 14.7°, 7.3° and 3.7°, respectively] are shown in Fig. 1 along with the MTA pixels. The original map has $N_{side} = 512$. The proximity of the MTA axis with one of the cold spots' center is evident.

In Table I, we show the directions in galactic coordinates of the four cosmic asymmetry axes. In Fig. 2, we show these directions in a Mollweide projection. The filled contours around each direction correspond to the 1σ error regions. In Table II, we show the corresponding angular separations for each pair.

The cumulative probability for obtaining a given value of MTA or larger may be obtained using 10^4 simulated statistically isotropic ΛCDM ILC maps [38]. The result

TABLE III. Probabilities of obtaining a simulated CMB map with a maximum temperature difference bigger than the observed one and with a MTA direction closer to the α dipole direction than the observed one.

	$\mathrm{MTA_{sims}} > \mathrm{MTA_{obs}}(\%)$	$\theta_{\mathrm{MTA}-\alpha,\mathrm{sims}} < \theta_{\mathrm{MTA}-\alpha,\mathrm{obs}}(\%)$	Both (%)
$N_{\mathrm{side}} = 4$	16.25	2.58	0.48
$N_{\mathrm{side}} = 8$	10.86	1.37	0.19
$N_{\mathrm{side}} = 16$	7.12	1.9	0.12

TABLE IV. Probabilities of obtaining a simulated CMB map with both a maximum temperature difference bigger than the observed one and a MTA direction closer than the observed one to the α, dark energy dipole and dark flow directions. The last column corresponds to the joint probability for obtaining a MTA axis closer to all the three other axes simultaneously. Due to the geometric arrangement of the axes, it is identical to the first column (see Fig. 2).

	$\alpha(\%)$	DE(%)	DF(%)	Joint α(%)-DE(%)-DF(%)
$N_{\mathrm{side}} = 4$	0.48	0.95	3.37	0.48
$N_{\mathrm{side}} = 8$	0.19	0.52	2.06	0.19
$N_{\mathrm{side}} = 16$	0.12	0.28	1.28	0.12

is shown in Fig. 3 for each one of the three angular resolutions (pixel sizes) considered. We used the publicly available ΛCDM simulated ILC maps of Ref. [38]. The observed value of the MTA magnitude is indicated by an arrow. The probability of obtaining the observed magnitude of MTA (or larger) in the context of ΛCDM varies between 16% and 7% depending on the ILC map's angular resolution. This result by itself does not indicate any statistically significant deviation from ΛCDM predictions. Perhaps this is the main reason that this simple statistic has been largely ignored by previous studies (see, however, Ref. [37]). However, the statistic becomes more interesting when the proximity of the direction of the MTA to other cosmic asymmetry axes is considered.

In Fig. 4, we plot the percentage of the MTA directions obtained from the simulated maps that form an angle with the observed α dipole direction smaller than a given angle (shown on the horizontal axis). The cases of map resolutions corresponding to $N_{\mathrm{side}} = 4$, 8, 16 are shown. The angle between the observed MTA and the *observed* α dipole direction is indicated by an arrow on each plot. In Figs. 5 and 6, we show the corresponding plots where instead of the α dipole direction we have used the dark energy dipole and dark flow directions, respectively.

The probability that the ΛCDM simulated maps reproduce the observed alignment of cosmic asymmetries varies between 1.37% (alignment with α dipole) and 22.77% (alignment with dark flow). The combined probability of obtaining both a large enough magnitude and angular proximity of MTA to the α dipole direction is shown in Table III. In particular, the probability of obtaining the observed MTA magnitude (or larger) and the observed angular proximity to the α dipole direction in the context of ΛCDM varies between 0.5% and 0.1% depending on the angular resolution of the WMAP7 ILC map. If the probability of obtaining the α dipole magnitude in the context of ΛCDM is also factored in, the probability reduces to about one part in 10^7, which is similar to the probability for simultaneously obtaining the dark energy and the α dipoles in the observed directions [10].

The last column of Table III is also shown in Table IV, along with the corresponding results for the other two anisotropy directions, corresponding to the dark energy dipole and the dark flow. The last column of Table IV corresponds to the joint probability for obtaining a MTA axis closer to all three other axes simultaneously. Due to the geometric arrangement of the axes, it is identical to the first column (see Fig. 2). This is because when the MTA axis comes closer to the α dipole axis, it is automatically closer to the other two axes.

We stress that the above abnormally low probabilities assume that the corresponding data sets (Keck + VLT quasar absorbers [9], dark flow data [4,6], Union2 data [39] and ILC maps [29]) are free of systematic errors. The potential validity of these data sets, combined with the generic nature of the statistical tests applied, assigns a particularly low likelihood to the statistical isotropy feature of ΛCDM.

Nevertheless, the existence of a physical model where the alignment of the above axes will appear with a significantly larger probability is a prerequisite before putting ΛCDM to disfavor. Even though the qualitative predictions of extended topological quintessence appear to be significantly more consistent with the observed cosmic asymmetries than ΛCDM, a quantitative analysis is required before any valid conclusion in favor of extended topological quintessence is drawn. Such an analysis is currently in progress.

III. CONCLUSION AND OUTLOOK

We have identified a direction on the maximum temperature asymmetry (MTA) of the WMAP7 foreground-reduced ILC map. Even though the magnitude of this asymmetry is consistent with ΛCDM at the 2σ level, its direction is abnormally close to other observed cosmic asymmetry axes. The direction of the MTA is close to the direction of one of the cold spots. This angular proximity may imply that this cold spot (or the opposite-located hot region) is physically related to the existence of other cosmic asymmetry axes. In the context of extended topological quintessence, the existence of such a feature (hot or cold spot) is expected at the core of the ''Great Repulser'' global defect, while in the opposite direction an opposite temperature behavior is expected.

The planarity and alignment of the CMB octupole and quadrupole moments may be partly due to a combination of two or more features on the preferred plane of these moments. Indeed, the MTA axis we have identified lies on this preferred plane, and therefore the MTA may be related to the observed quadrupole-octupole alignment [16].

An interesting extension of this project is the derivation of the detailed CMB signature predicted by Extended Topological Quintessence. Such a derivation would involve a cosmological simulation of the evolution of the non-minimally coupled $O(3)$ scalar field that gives rise to the recent formation global defect. The linear metric perturbations that emerge due to this formation can then be numerically calculated [40], and the corresponding ISW effect can be derived in a straightforward manner. This numerical analysis can also lead to detailed predictions about the magnitude and geometry of the other cosmic asymmetry axes (dark flow, dark energy and α dipole). This analysis is currently in progress.

Numerical analysis files: The data, Mathematica and HEALPix program files used for the numerical analysis may be downloaded from Ref. [41].

ACKNOWLEDGMENTS

We acknowledge the use of the Legacy Archive for Microwave Background Data Analysis (LAMBDA) [42] and the use of the HEALPix package [34]. This research has been cofinanced by the European Union (European Social Fund; ESF) and Greek national funds through the Operational Program ''Education and Lifelong Learning'' of the National Strategic Reference Framework (NSRF) Research Funding Program ARISTEIA, investing in the society of knowledge through the European Social Fund.

[1] P. Zhang and A. Stebbins, Phys. Rev. Lett. **107**, 041301 (2011).
[2] I. Antoniou and L. Perivolaropoulos, J. Cosmol. Astropart. Phys. 12 (2010) 012.
[3] L. Perivolaropoulos, arXiv:0811.4684.
[4] R. Watkins, H. A. Feldman, and M. J. Hudson, Mon. Not. R. Astron. Soc. **392**, 743 (2009); H. A. Feldman, R. Watkins, and M. J. Hudson, Mon. Not. R. Astron. Soc. **407**, 2017 (2010).
[5] G. Lavaux, R. B. Tully, R. Mohayaee, and S. Colombi, Astrophys. J. **709**, 483 (2010).
[6] A. Kashlinsky, F. Atrio-Barandela, D. Kocevski, and H. Ebeling, Astrophys. J. **686**, L49 (2008); A. Kashlinsky, F. Atrio-Barandela, and H. Ebeling, arXiv:1202.0717; A. Kashlinsky, F. Atrio-Barandela, H. Ebeling, A. Edge, and D. Kocevski, Astrophys. J. **712**, L81 (2010); F. Atrio-Barandela, A. Kashlinsky, H. Ebeling, and D. Kocevski, arXiv:1211.4345.
[7] D.-C. Dai, W. H. Kinney, and D. Stojkovic, J. Cosmol. Astropart. Phys. 04 (2011) 015; J. Colin, R. Mohayaee, S. Sarkar, and A. Shafieloo, Mon. Not. R. Astron. Soc. **414**, 264 (2011).
[8] C. Tsagas, Mon. Not. R. Astron. Soc. **405**, 503 (2010).
[9] J. K. Webb, J. A. King, M. T. Murphy, V. V. Flambaum, R. F. Carswell, and M. B. Bainbridge, Phys. Rev. Lett. **107**, 191101 (2011); J. A. King, J. K. Webb, M. T. Murphy, V. V. Flambaum, R. F. Carswell, M. B. Bainbridge, M. R. Wilczynska, and F. E. Koch, arXiv:1202.4758.
[10] A. Mariano and L. Perivolaropoulos, Phys. Rev. D **86**, 083517 (2012).
[11] J. C. B. Sanchez and L. Perivolaropoulos, Phys. Rev. D **84**, 123516 (2011).
[12] A. Vilenkin, Phys. Rev. Lett. **72**, 3137 (1994); A. D. Linde, Phys. Lett. B **327**, 208 (1994); N. Sakai, H.-A. Shinkai, T. Tachizawa, and K.-i. Maeda, Phys. Rev. D **53**, 655 (1996); **54**, 2981(E) (1996); I. Cho and A. Vilenkin, Phys. Rev. D **56**, 7621 (1997); A. A. de Laix, M. Trodden, and T. Vachaspati, Phys. Rev. D **57**, 7186 (1998).
[13] M. Cruz, N. Turok, P. Vielva, E. Martinez-Gonzalez, and M. Hobson, Science **318**, 1612 (2007).
[14] C. J. Copi, D. Huterer, D. J. Schwarz, and G. D. Starkman, Adv. Astron. **2010**, 847541 (2010).
[15] C. L. Bennett, R. S. Hill, G. Hinshaw, D. Larson, K. M. Smith, J. Dunkley, B. Gold, and M. Halpern *et al.*, Astrophys. J. Suppl. Ser. **192**, 17 (2011).
[16] M. Tegmark, A. de Oliveira-Costa, and A. Hamilton, Phys. Rev. D **68**, 123523 (2003); A. de Oliveira-Costa and M. Tegmark, Phys. Rev. D **74**, 023005 (2006); J. P. Ralston and P. Jain, Int. J. Mod. Phys. D **13**, 1857 (2004).
[17] D. J. Schwarz, G. D. Starkman, D. Huterer, and C. J. Copi, Phys. Rev. Lett. **93**, 221301 (2004).
[18] C. L. Bennett *et al.* (WMAP Collaboration), Astrophys. J. Suppl. Ser. **148**, 1 (2003).
[19] M. Cruz, L. Cayon, E. Martinez-Gonzalez, P. Vielva, and J. Jin, Astrophys. J. **655**, 11 (2007).
[20] P. Mukherjee and Y. Wang, Astrophys. J. **613**, 51 (2004).

[21] D. N. Spergel *et al.* (WMAP Collaboration), Astrophys. J. Suppl. Ser. **148**, 175 (2003).
[22] C. J. Copi, D. Huterer, D. J. Schwarz, and G. D. Starkman, Mon. Not. R. Astron. Soc. **399**, 295 (2009).
[23] Y. Ayaita, M. Weber, and C. Wetterich, Phys. Rev. D **81**, 023507 (2010).
[24] A. Hajian, arXiv:astro-ph/0702723.
[25] J. Kim and P. Naselsky, Astrophys. J. **724**, L217 (2010); **739**, 79 (2011).
[26] J. Hoftuft, H. K. Eriksen, A. J. Banday, K. M. Gorski, F. K. Hansen, and P. B. Lilje, Astrophys. J. **699**, 985 (2009).
[27] F. Finelli, A. Gruppuso, F. Paci, and A. A. Starobinsky, J. Cosmol. Astropart. Phys. 07 (2012) 049.
[28] K. Land and J. Magueijo, Phys. Rev. D **72**, 101302 (2005).
[29] N. Jarosik, C. L. Bennett, J. Dunkley, B. Gold, M. R. Greason, M. Halpern, R. S. Hill, and G. Hinshaw *et al.*, Astrophys. J. Suppl. Ser. **192**, 14 (2011).
[30] E. D. Kovetz, A. Ben-David, and N. Itzhaki, Astrophys. J. **724**, 374 (2010).
[31] L. Ackerman, S. M. Carroll, and M. B. Wise, Phys. Rev. D **75**, 083502 (2007); **80**, 069901(E) (2009).
[32] J. F. Donoghue, K. Dutta, and A. Ross, Phys. Rev. D **80**, 023526 (2009).
[33] A. L. Erickcek, M. Kamionkowski, and S. M. Carroll, Phys. Rev. D **78**, 123520 (2008).
[34] K. M. Gorski, E. Hivon, A. J. Banday, B. D. Wandelt, F. K. Hansen, M. Reinecke, and M. Bartelman, Astrophys. J. **622**, 759 (2005).
[35] J. Grande and L. Perivolaropoulos, Phys. Rev. D **84**, 023514 (2011).
[36] H. Alnes and M. Amarzguioui, Phys. Rev. D **74**, 103520 (2006).
[37] P. Naselsky, M. Hansen, and J. Kim, J. Cosmol. Astropart. Phys. 09 (2011) 012.
[38] H. K. Eriksen, A. J. Banday, K. M. Gorski, and P. B. Lilje, arXiv:astro-ph/0508196; http://lambda.gsfc.nasa.gov/product/map/dr1/hke_ILC_get.cfm.
[39] R. Amanullah *et al.*, Astrophys. J. **716**, 712 (2010).
[40] D. P. Bennett and S. H. Rhie, Astrophys. J. **406**, L7 (1993).
[41] http://leandros.physics.uoi.gr/mta.
[42] http://lambda.gsfc.nasa.gov/.